Exchange coupling in NiO/CoFe2 and CoFe2O4/CoFe2 systems grown by pulsed laser deposition

T. Fix, S. Colis, K. Sauvet, J.-L. Loison, G. Versini, G. Pourroy, A. Dinia

Exchange coupling in $NiO/CoFe_2$ and $CoFe_2O_4/CoFe_2$ systems grown by pulsed laser deposition

T. Fix,[a] S. Colis, K. Sauvet, J. L. Loison, G. Versini, G. Pourroy, and A. Dinia
Institut de Physique et Chimie des Matériaux de Strasbourg (IPCMS), Unité Mixte de Recherche 7504 du Centre National de la Recherche Scientifique (CNRS), Ecole Européenne de Chimie, Polymères et Matériaux de Strasbourg (ECPM), Université Louis Pasteur, 23 Rue du Loess BP43 F-67034 Strasbourg, France

(Received 23 June 2005; accepted 3 January 2006; published online 28 February 2006)

$NiO(30\ nm)/CoFe_2(5\ nm)$ bilayers are grown by pulsed laser deposition on Si (001). After annealing under a magnetic field we observe an exchange bias of −86 Oe, corresponding to an exchange coupling of 0.06 erg/cm^2. While a similar exchange coupling is observed in $NiO(30\ nm)/CoFe_2(5\ nm)/SrTiO_3(3\ nm)/Ni_{80}Fe_{20}(5\ nm)/Ta(5\ nm)$, the stack $SFMO(30\ nm)/SrTiO_3(3\ nm)/CoFe_2(5\ nm)/NiO(30\ nm)/Ta(5\ nm)$ does not provide any exchange bias with NiO on the top electrode. Alternatively, we have used a ferrimagnetic oxide ($CoFe_2O_4$) as a bias layer of the top electrode. The stack $SFMO(30\ nm)/STO(3\ nm)/CoFe_2(5\ nm)/CoFe_2O_4(70\ nm)$ provides a shift of −70 Oe for the $CoFe_2(5\ nm)$ layer, corresponding to an exchange coupling of 0.05 erg/cm^2. © *2006 American Institute of Physics*. [DOI: 10.1063/1.2173045]

I. INTRODUCTION

Several techniques are employed for the growth of thin films and multilayers, such as sputtering, molecular beam epitaxy (MBE), chemical vapor deposition (CVD), and pulsed laser deposition (PLD). PLD, also sometimes called laser MBE, was popularized in the late 1980s through its success in depositing epitaxial high temperature superconducting films.[1] This technique consists in focusing an intense laser pulse on the surface of a target, creating a plasma that expands and allows the growth of thin films. PLD is a very versatile technique that allows the growth of complex materials such as metallic alloys, semiconductors, and oxide thin films. One of the advantages of PLD is that thin films of complex multicomponent materials, such as Sr_2FeMoO_6 (SFMO), can be obtained with the preservation of the stoichiometry of the target material. Nevertheless, the use of PLD for the growth of multilayers has been very limited so far, especially in the field of spintronics, probably due to the maturity of the other techniques and also because of the small deposition areas imposed and the problem of droplet deposition. In this paper we show with two examples that PLD seems to be adapted for the growth of thin films and multilayers in the field of spintronics.

In spin-valve structures and magnetic tunnel junctions, an antiparallel magnetization of the two ferromagnetic layers separated by a nonmagnetic spacer is obtained when the hard and soft layers provide quite different coercive fields. The larger the difference of coercive fields, the more suited the system for integration in magnetoelectronic devices. Therefore, a coercive field of the hard layer as large as possible is needed. This is often achieved by coupling a ferromagnetic and an antiferromagnetic layer through exchange anisotropy. Exchange anisotropy or exchange bias is an effect evidenced by Meiklejohn and Bean.[2] It consists in a shift of the hysteresis loop of a ferromagnetic/antiferromagnetic bilayer.

In this paper we focus on SFMO-based magnetic tunnel junctions using two exchange bias layers, NiO and $CoFe_2O_4$, for the hard electrode. NiO films provide a high chemical stability and a high blocking temperature (around 500 K).[3,4] Exchange coupling with NiO has been observed in sputtered NiO/Co (Refs. 5 and 6) and NiO/NiFe (Refs. 6–8) systems. $CoFe_2O_4$ is a good ferrimagnet with a Curie temperature of 793 K. It shows as well a good chemical stability but presents the advantage of aligning its magnetic moments in an external field without annealing.[9]

II. EXPERIMENT AND RESULTS

The samples are grown at 120 °C on Si (001) by pulsed laser deposition, using a KrF laser with a 10 Hz repetition rate and a fluence of 1 J/cm^2 on the target. NiO films are grown from a Ni metal target in 20% O_2+N_2 at a pressure of 10^{-3} mbar. After deposition the samples are annealed up to 270 °C for 20 min in an Ar atmosphere and then cooled down to room temperature in a magnetic field of 10 kOe in order to set the exchange coupling. The film thickness is calibrated by x-ray grazing angle reflectometry. Magnetic measurements are carried out at room temperature with an alternating gradient field magnetometer (AGFM), with the magnetic field applied in the film plane. Figure 1 shows the magnetization curve of a $NiO(30\ nm)/CoFe_2(5\ nm)$ bilayer before and after annealing. Before annealing one can distinguish a switching in two steps of the magnetization, while only one step is observed after annealing the sample under a magnetic field. Before annealing the two steps of the magnetization curve are due to the Ni metallic clusters inside the NiO layer which reverse their magnetization at low fields (close to zero) and to the $CoFe_2$ layer which switches the magnetization at higher fields (around 200 Oe). Indeed, during the laser ablation of the Ni target, clusters of Ni can be

[a]Author to whom correspondence should be addressed; FAX: +33 (0)3 88 10 72 47; electronic mail: thomas.fix@ipcms.u-strasbg.fr

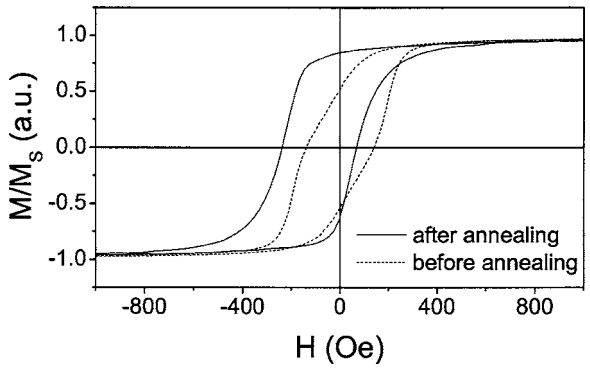

FIG. 1. Magnetization curve before and after annealing of a NiO(30 nm)/$CoFe_2$(5 nm) bilayer at 300 K.

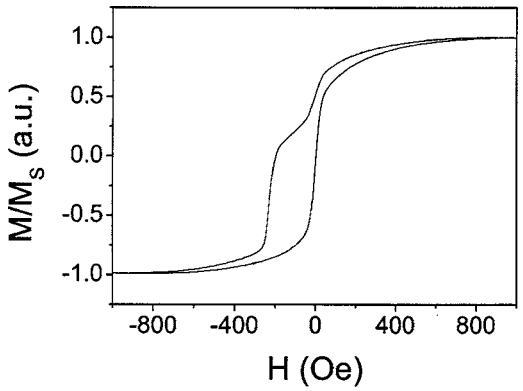

FIG. 2. Magnetization curve of the following stack: NiO(30 nm)/$CoFe_2$(5 nm)/$SrTiO_3$(3 nm)/$Ni_{80}Fe_{20}$(5 nm)/Ta(5 nm) at 300 K.

ejected from the target and deposited on the substrate. In these conditions, there are two ways of incorporating oxygen in the NiO layer. First, oxygen can react with the Ni cluster surface, forming NiO (which is a thermodynamically stable process). Second, oxygen can be physically trapped by clusters that arrive at the film surface (which is a thermodynamically unstable process). This leads therefore to an oxygen excess at the boundaries between clusters. If the cluster size is small (since the roughness of such NiO layer is very small), one can easily imagine that the excess of oxygen trapped at the cluster interface is sufficient to oxidize the metallic Ni inside the clusters after annealing. As a consequence only one reversal step is observed on the magnetization loop which is due solely to the magnetization of the $CoFe_2$ layer. The NiO layer is now homogeneous all over the thickness, is free of Ni metallic clusters, and presents a well defined antiferromagnetic character. This can be easily seen on the magnetization curve of the annealed sample which provides a shift of the hysteresis loop. An exchange bias of −86 Oe is evidenced, which corresponds to an exchange coupling of 0.06 erg/cm^2. This value is close to the ones obtained in sputtered NiO/Co (Ref. 6) and NiO/NiFe (Ref. 8) systems. X-ray diffraction (XRD) spectra obtained using a two-circle Siemens D500 diffractometer (Co $K_{\alpha 1}$ radiation) indicate that NiO is textured along the (111) direction.

Furthermore, the NiO/$CoFe_2$ hard layer is integrated in a hard-soft system. The following stack is grown by pulsed laser deposition on Si(001):NiO(30 nm)/$CoFe_2$(5 mm)/$SrTiO_3$(3 nm)/$Ni_{80}Fe_{20}$(5 nm)/Ta(5 nm), where $SrTiO_3$(3 nm) is a tunnel barrier and Ta a protection capping. Layers of Ta, $SrTiO_3$ (STO), and $CoFe_2$ are grown with the same fluence of 1 J/cm^2 at room temperature in vacuum. No SFMO was used as upper soft electrode since its preparation requires high deposition temperatures (~800 °C) which leads to a complete interdiffusion of the hard electrode and the STO barrier. Figure 2 shows the magnetization curve obtained for this stack. Decreasing the field from saturation, the $Ni_{80}Fe_{20}$(5 nm) layer switches its magnetization around 0 Oe, followed at about −230 Oe by the switching of the $CoFe_2$(5 nm) layer. The high switching field of the $CoFe_2$ magnetization is obtained owing to the exchange anisotropy created at the interface between NiO and $CoFe_2$. When we go back from negative to positive fields, the exchange bias shifts the switching field of $CoFe_2$ to reach coincidentally the switching field value of the $Ni_{80}Fe_{20}$ layer. This leads to a single switching step of the magnetization rotation instead of to the two steps observed when coming from the positive saturation.

We tried as well to use the NiO/$CoFe_2$ bilayer as a top hard electrode by integrating it in a more difficult hard-soft system based on a SFMO double perovskite. SFMO is a promising candidate for spin-polarized transport applications due to its half metallic properties. It provides a high spin polarization[10–12] combined with a high Curie temperature of 415 K.

SFMO layers are grown epitaxially from a sintered SFMO target at 800 °C on STO (001) with the same pulsed laser deposition configuration as described above. Our films are grown in 20% O_2+N_2 at a pressure of 4×10^{-6} mbars. More details on the preparation of our SFMO samples are given elsewhere.[13,14] We obtain samples with a Curie temperature above 400 K, a root-mean-square roughness of 0.3 nm, areas without splashing as large as 100 μm^2, and a maximum magnetization of 3.4 μB/f.u. at 5 K. Figure 3(a) shows that SFMO films are, at room temperature, neither good magnetic soft layers nor good hard layers. They provide a low coercive field and a low remanence combined with a high saturation field of around 10 kOe and a low squareness. The low squareness and low coercitivity are related to thermal activation correlated with the size and anisotropy distribution of the crystalline grains. As a consequence, some magnetic grains rotate their magnetization before the others. The smaller grains turn first their magnetic moments followed by the largest grains. The change in magnetization is purely rotational due to the small grain size. This is in agreement with the absence of contrast observed by magnetic force microscopy measurements made under variable

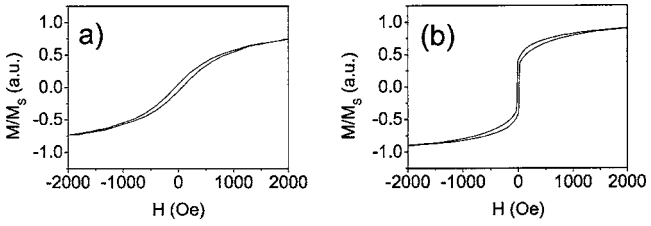

FIG. 3. Magnetization curve of (a) SFMO (30 nm) and (b) SFMO(30 nm)/$SrTiO_3$(3 nm)/$CoFe_2$(5 nm)/Ta(5 nm) at 300 K.

magnetic field which emphasizes the fact that there is no correlation between the moments. The high saturation field can be explained by the fact that there are grains which have sizes close to the superparamagnetic regime.

If we try to integrate SFMO in the stack SFMO(30 nm)/$SrTiO_3$(3 nm)/$CoFe_2$(5 nm)/Ta(5 nm), we observe in Fig. 3(b) a slow reversal which represents 60% of the total magnetization and a sharp reversal of 40% of the total magnetization. Assuming a magnetization of around 1400 emu/cm^3 for $CoFe_2$ and 300 emu/cm^3 for SFMO we obtain a magnetic contribution of 44% for $CoFe_2$ and 56% for SFMO. Considering the shape of the magnetization loop of SFMO shown in Fig. 3(a), we can therefore assume that the slow and sharp reversals are due solely to SFMO and $CoFe_2$, respectively. The reversal of $CoFe_2$ occurs around ±10 Oe. Therefore, a full antiparallel configuration of SFMO and $CoFe_2$ is never reached, so that we need a good pinning layer. A further difficulty is that SFMO has to be grown at high temperatures on STO (001) so that the pinning layer must be on the upper electrode and cannot be grown directly on the substrate.

We have first tried the NiO exchange bias layer in the stack SFMO(30 nm)/$SrTiO_3$(3 nm)/$CoFe_2$(5 nm)/NiO(30 nm)/Ta(5 nm). Unfortunately, the magnetization curve did not show any exchange bias. It is well known that the exchange bias is very sensitive to the roughness and the texture of the antiferromagnetic layer. Therefore the nature of the layer on which NiO has to be deposited is very important. It seems in our case that the $CoFe_2$ layer did not give an appropriate surface for the (111) texture of NiO.

We have then tried another hard magnetic system: $CoFe_2/CoFe_2O_4$. $CoFe_2O_4$ layers are obtained with a $CoFe_2$ target in 20% O_2+N_2 at a pressure of 10^{-3} mbar. More details on $CoFe_2/CoFe_2O_4$ bilayers are given elsewhere.[9]

The following stack is grown by PLD: SFMO(30 nm)/STO(3 nm)/$CoFe_2$(5 nm)/$CoFe_2O_4$(70 nm), where SFMO is the bottom electrode and $CoFe_2$(5 nm)/$CoFe_2O_4$(70 nm) is the top electrode. Figure 4(a) shows the magnetic curve of this stack. Coming from the positive saturation we observe first the beginning of the reversal of the SFMO magnetization. This is followed by a sudden magnetization drop around −300 Oe which corresponds to the reversal of the $CoFe_2$ magnetization. Finally, the $CoFe_2O_4$ and SFMO magnetizations rotate progressively until the saturation at around −20 kOe. In order to evidence the magnetization loop shift we zoom in the zero-field region in Fig. 4(b). We observe that the $CoFe_2$ layer is pinned by the

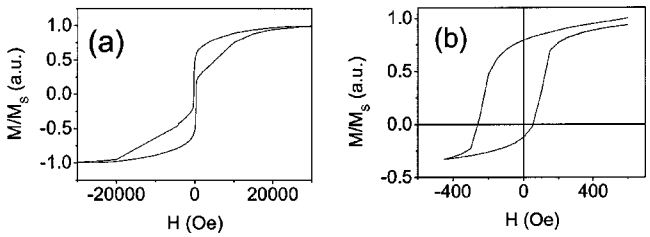

FIG. 4. (a) Magnetization curve at 300 K of SFMO(30 nm)/STO(3 nm)/$CoFe_2$(5 nm)/$CoFe_2O_4$(70 nm); (b) minor loop of this stack.

$CoFe_2O_4$ layer since the $CoFe_2$ magnetization starts to turn around −250 Oe instead of −10 Oe [Fig. 3(b)]. In addition the magnetization loop is not symmetric with respect to the zero field but is shifted by a value of −70 Oe. This corresponds to an exchange coupling of 0.05 erg/cm^2.

III. CONCLUSION

In summary, we show that exchange bias can be obtained by pulsed laser deposition. We obtain an exchange coupling of 0.06 and 0.05 erg/cm^2 for NiO/$CoFe_2$ and $CoFe_2/CoFe_2O_4$ systems, respectively. No coupling is observed when NiO is integrated in the top hard electrode, while a coupling is observed when, instead of NiO, a $CoFe_2O_4$ ferrimagnetic layer is used.

ACKNOWLEDGMENTS

The authors thank G. Dekyndt and G. Schmerber for technical assistance. This work was supported by the Region Alsace, France.

[1] D. Dijkkamp, T. Venkatesan, X. D. Wu, S. A. Shaheen, N. Jisrawi, Y. H. Min-Lee, W. L. Mclean, and M. Croft, Appl. Phys. Lett. **51**, 619 (1987).
[2] W. H. Meiklejohn and C. P. Bean, Phys. Rev. **102**, 1413 (1956).
[3] T. Nagamiya, K. Yosida, and R. Kubo, Adv. Phys. **4**, 2 (1955).
[4] D. H. Han, J. G. Zhu, and J. H. Judy, J. Appl. Phys. **81**, 4996 (1997).
[5] J. F. Bobo, S. Dubourg, E. Snoeck, B. Warot, P. Baules, and J. C. Ousset, J. Magn. Magn. Mater. **206**, 118 (1999).
[6] L. Smardz, J. Magn. Magn. Mater. **240**, 273 (2002).
[7] M. J. Carey and A. E. Berkowitz, Appl. Phys. Lett. **60**, 3061 (1992).
[8] A. Paetzold and K. Röll, J. Appl. Phys. **91**, 7748 (2002).
[9] N. Viart, R. Sayed Hassan, J. L. Loison, G. Versini, F. Huber, P. Panissod, C. Mény, and G. Pourroy, J. Magn. Magn. Mater. **279**, 21 (2004).
[10] K. I. Kobayashi, T. Kimura, H. Sawada, K. Terakura, and Y. Tokura, Nature (London) **395**, 677 (1998).
[11] M. Besse *et al.*, Europhys. Lett. **60**, 608 (2002).
[12] M. Bibes *et al.*, Appl. Phys. Lett. **83**, 2629 (2003).
[13] T. Fix, G. Versini, J. L. Loison, S. Colis, G. Schmerber, G. Pourroy, and A. Dinia, J. Appl. Phys. **97**, 024907 (2005).
[14] T. Fix, D. Stoeffler, S. Colis, C. Ulhaq, G. Versini, J. P. Vola, F. Huber, and A. Dinia, J. Appl. Phys. **98**, 023712 (2005).